

# Melt Instabilities and the Effect of Surface Tension on Preventing Edge Serrations in Melt Overflow Alloy Strip Casting

Ali KALKANLI, John V. WOOD<sup>1)</sup> and Nicholas BRAITHWAITE<sup>2)</sup>

Middle East Technical University, Department of Metallurgical and Materials Engineering, Inonu Bulvarı 06531 Ankara, Turkey.  
 1) The University of Nottingham, Materials Engineering and Materials Design, University Park NG7, Nottingham, United Kingdom.  
 2) The Open University, Faculty of Technology, Materials Discipline, Milton Keynes, MK7 6AA, United Kingdom.

(Received on June 11, 1997; accepted in final form on October 2, 1997)

Direct casting of metallic strip onto a single rotating chiller is possible by the displacement of liquid metal in a horizontal pouring channel against a vertically moving chiller surface. In the case where of a high liquid/vapour surface tension exists, the liquid cannot be dragged out of the melt pool by momentum transfer. The critical surface tension values for making strip in a series of 304 stainless steels as measured by a modified oscillating droplet technique, values 2.1–1.4 N m<sup>-1</sup>. Surface tension values greater than these lead strip breakup. Casting of alloys with a low surface tension such as 1.3–1.1 N m<sup>-1</sup> at a wheel speed of 2.7 m s<sup>-1</sup> can result instability waves such as Marangoni, Kelvin–Helmholtz and capillary waves. These waves result in the formation of edge serrations in the solidified strip. If the casting speed is sufficiently high to overcome these melt instabilities, strips can be produced with a smooth edge and uniform dimensions. In this paper the results of melt overflow direct strip casting experiments with different alloy and process conditions for strip dimensions up to 700 μm and 40 mm wide are presented.

KEY WORDS: melt instabilities; Kelvin Helmholtz instability; capillary waves; Marangoni instability; surface tension; casting speed.

## 1. Introduction

In this study the results of experimental work concerning the verification of melt overflow direct strip casting technique for making reproducible strip are compared with the theoretical models needed to explain strip edge serrations and dimensional nonuniformities originating from original liquid surface disturbance during casting. The melt overflow technique<sup>1)</sup> was employed to produce 304 stainless steel strip. A series of 304 stainless steels with different sulphur contents were prepared to investigate the effect of different liquid surface tension values of the alloy on the final strip characteristics.

Direct casting of liquid metal onto a rotating chiller requires special conditions for producing continuous strips. Maintaining and providing laminar liquid flow in the melt pool delivered to the casting wheel is one of the important parameters for sound strip production.<sup>2)</sup> It is known that lateral variations in the thickness of a ribbon are directly related to the pool shape at a given instant in time. Longitudinal dimensional variations in the thickness or width of the strip indicate an unstable melt pool. These dimensional variations can be minimized by using confined nozzles or lip configurations, optimum liquid delivery velocities, and pool dimensions that induce uniformity and steadiness in the fluid flow, optimum alloy

composition to control the surface tension of the flow and minimum gap between rotary chiller and furnace lip in order to minimize draught effects.

## 2. Process Description

A schematic diagram of the melt overflow strip casting technique is shown in **Fig. 1**. Liquid metal is displaced through an open channel onto the rotating chiller surface. The chiller speed was kept constant as 2.78 m s<sup>-1</sup>. The furnace lip is placed at a small distance maintaining 0.5 mm gap with the rotary chiller having a diameter of 270 mm. The induction furnace capable of melting 5 kg of stainless steel charge was positioned at an angle 38° with horizontal and liquid metal was poured through an open refractory channel having 50 mm width and 22–35 mm varying depth. Liquid metal temperatures measured before delivery were in 1 600–1 700°C temperature range to provide sufficient fluidity during delivery. A series of 304 stainless alloys were prepared keeping O concentration in the range of % 0.01–0.03 by FeSi deoxidation. FeS was added to vary the %S in the range of 0.01–0.07 to control surface tension. The water cooled chiller surface temperature was approximately 25°C and it was close to the hot liquid stream at 1 700°C flowing through the channel (**Fig. 2**). This resulted in large temperature gradients and subsequent surface tension

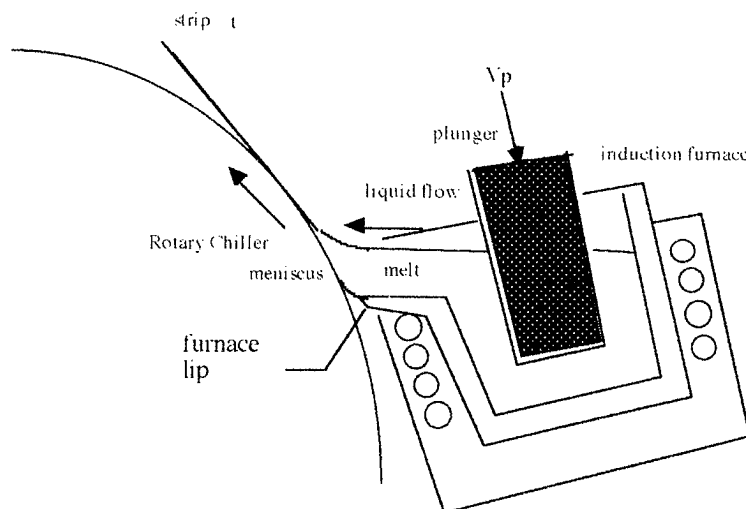


Fig. 1. Schematic diagram of melt overflow strip casting.

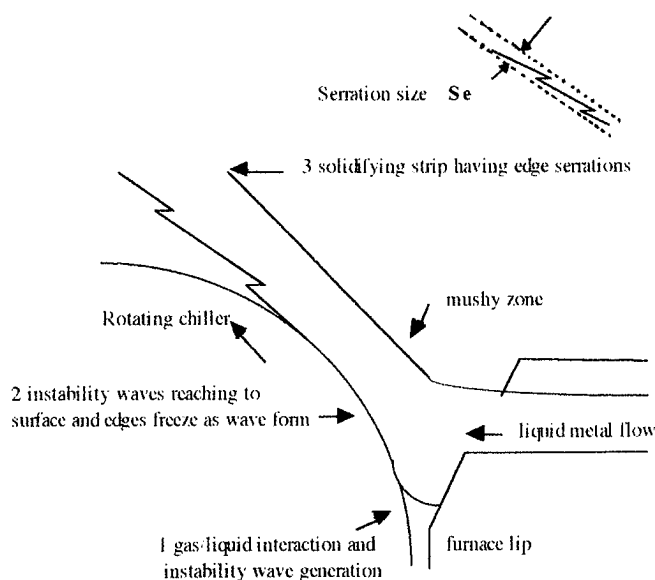


Fig. 2. Schematic diagram of strip edge serration formation.

gradients in the liquid stream. Liquid metal having speed of about  $3\text{--}5\text{ cm s}^{-1}$  is displaced by the inert plunger travelling down with speed of  $3.70\text{ mm s}^{-1}$  and overflows the lip, onto the rotating chiller where it solidifies and leaves the wheel.

### 3. Theoretical Considerations

Strip nonuniformities and edge serrations are caused by hydrodynamic instabilities developed within the melt pool. Hydrodynamic instabilities in the melt pool originate from the interaction between the thin gas boundary layer on the chiller and the flowing liquid metal strip just at the point of contact. Figure 2 shows the possible effects of instability waves near the edges schematically. These waves also reach to the free flat surface and deteriorate the free side surface quality. The effects of these instabilities on the meniscus need to be controlled if a satisfactory strip is to be cast. The major melt instabilities can be classified as;

(1) “Capillary waves” Levich<sup>4)</sup> describes such a wave motion which penetrates only to a depth of the order of one wavelength.

(2) Kelvin-Helmholtz instabilities<sup>2)</sup> which arises at the interface between differentially moving fluids.

(3) Marangoni instabilities<sup>5)</sup> which cause bulk flow arising from local variations of surface tension.

Such waves may arise from random perturbations generated by any source. They may occur as a result of turbulence within the melt puddle or from the gas boundary layer eddying on the surface.

#### 3.1. Capillary Waves

The velocity difference between the rotary chiller and liquid metal stream can determine the conditions which may promote perturbations in the liquid state the high stream velocities may cause turbulent flow of the liquid and splashing.<sup>6)</sup> As the liquid metal stream travels from the lip to the moving chilled substrate standing or travelling capillary waves can also form in the liquid stream. These waves are initiated at sources generally at the meniscus of the lip during melt overflow. In addition, capillary waves can be generated along the melt stream by the interaction with the atmosphere analogous to the formation of capillary wind wave on a lake. The velocity of capillary waves  $C_\lambda$  of wavelength  $\lambda$  is determined from a balance between inertia forces and surface tension  $\sigma_{lv}$ .<sup>7)</sup> The minimum stream velocity  $V_j$  required to overcome these instabilities can be given as;

$$V_j \geq \sqrt{\frac{\sigma_{lv}}{R_j \rho}} \dots\dots\dots (1)$$

where  $R_j$  is liquid stream radius,  $\rho$  is density of liquid metal and  $\sigma_{lv}$  is surface tension. The stream velocity must be large enough to overcome any instabilities developing in the stream otherwise the impingement of these instabilities on the pool near the wheel would cause a time variation in the puddle size and subsequent variations in the strip dimensions. Rayleigh,<sup>9)</sup> has shown that the amplitude  $k$  of the fastest growing instability increases with time as;

$$k = k_0 \exp(q\theta) \dots\dots\dots(2)$$

$$q = 0.34 \sqrt{\frac{\sigma_{lv}}{\rho R_j^3}} \dots\dots\dots(3)$$

where  $k_0$  is the initial amplitude of the instability,  $\theta$  is the time since the initiation of the instability. For a stream length  $L_j$  moving at a velocity  $V_j$ , the time available for an instability to grow will be of the order of  $\theta$ . Then Eq. (3) and the fact that  $\theta$  together yield the minimum stream velocity  $V_j$ , required to suppress growth of remain unwashed capillary instabilities on stream. Substituting  $\theta = L_j/V_j$  in Eq. (2) we can obtain a combined equation for  $V_j$ . We take ln of both sides and it yields the equation as follows;

$$\ln(k/k_0) = \frac{0.34L_j}{V_j} \left( \sqrt{\frac{\sigma_{lv}}{R_j^3 \rho}} \right) \dots\dots\dots(4)$$

after rearranging this equation to obtain  $V_j$  it finally appears as;

$$V_j = \frac{0.34L_j}{\ln(k/k_0)} \left( \sqrt{\frac{\sigma_{lv}}{R_j^3 \rho}} \right) \dots\dots\dots(5)$$

considering the increase of amplitude of an instability is limited to a factor of 10 from its very small initial value. Thus,

$$V_j \geq \frac{L_j}{\ln(10)} \left( \sqrt{\frac{\sigma_{lv}}{R_j^3 \rho}} \right) \dots\dots\dots(6)$$

It has been reported by Anthony and Cline,<sup>3)</sup> that excessive stream velocities should be avoided to prevent turbulence. So a critical condition is verified in order to reach a balance and maintain a steady liquid flow. This critical condition will be governed by process parameters such as stream length  $L_j$ , stream diameter  $R_j$  and also by alloy characteristics such as surface tension and density.

**3.2. Kelvin–Helmholtz Instability**

The Kelvin–Helmholtz (KH) instability arises as a result of the pressure perturbation exerted by the gas which is accelerated by the rotating chill wheel. This can do work on the liquid strip/gas interface and at a sufficiently large relative or differential velocity the instability can tear apart the molten film. The agreement is good between experiments and Kelvin–Helmholtz instability predictions as determined by experiments on high viscosity materials such as molten metals.<sup>11)</sup> Nayfeh and Saric<sup>13)</sup> reported that at a low liquid Reynold’s number and with subsonic gas flow, stability conditions are independent of viscosity. In a linear analysis, the nonlinear motion of the gas has no effect and the nonlinear motion of the viscous liquid is stabilized. The instability condition predicted numerically for two uniform fluid half planes in relative vertical motion separated by a vertical boundary with stream velocities  $V_1$  and  $V_2$ , densities  $\rho_1$  and  $\rho_2$  are constant.<sup>14)</sup> The stabilizing effect of surface tension  $\sigma$  on the KH instability is expressed by

$$(V_1 - V_2)^2 < \frac{2}{a_1 a_2} \sqrt{\frac{\sigma_{lv} g (a_1 - a_2)}{\rho_1 + \rho_2}} \dots\dots\dots(7)$$

where  $\rho$  is density,  $a_1$  and  $a_2$  are ratios of densities of interacting fluids

$$a_1 = \frac{\rho_1}{\rho_1 + \rho_2}, \quad a_2 = \frac{\rho_2}{\rho_1 + \rho_2}$$

$V_1 - V_2 = 6.5 \text{ m s}^{-2}$  was reported for the stability condition for air flowing over water by Chandrasekhar.<sup>14)</sup> When velocity difference  $\Delta V$  exceeded  $6.5 \text{ m s}^{-1}$  instability manifested itself as surface waves with a wavelength 17.1 mm for the conditions he investigated.

**3.3. Marangoni Instability in Liquid Pool**

Surface tension gradients coupled with the additional stirring from the induction coil generate thermocapillary flow and convection in the melt channel.

The Marangoni number Ma is a ratio of convective heat flow to conductive heat flow. The following definition of Marangoni number can be written as;

$$\text{Ma} = \frac{V \rho C_p \Delta T}{K \frac{\partial T}{\partial x}} \dots\dots\dots(8)$$

where  $\rho C/K = 1/\alpha$ ,  $K$  is thermal conductivity,  $\alpha$  is thermal diffusivity,  $C_p$  is specific heat,  $y$  is pool dimension or length scale for surface temperature gradient,  $\Delta T$  temperature difference,  $\gamma$  is temperature coefficient of surface tension and horizontal velocity,  $V = \gamma \cdot \partial T / \partial x \cdot y / \mu$  after substituting  $V$  and  $\alpha$  in Eq. (8) it appears as;

$$\text{Ma} = \frac{\gamma \Delta T y}{\alpha \mu} \dots\dots\dots(9)$$

where  $\mu$  is viscosity, convective heat flow =  $V \rho c \Delta T$ , conductive heat flow =  $K \cdot \partial T / \partial x$ . In a heat transfer system, the measure of the intensity of convection relative to conduction is described by the Peclet number. The Peclet number (Pe) is based on a thermocapillary reference velocity also denoted as the Marangoni number (Ma) which is the basic dimensional parameter of thermocapillary convection. Assuming  $y$  is equal to liquid pool width Ma can be written as:

$$\text{Ma} = \text{Pe} = \frac{\gamma \Delta T D}{\mu \alpha} \dots\dots\dots(10)$$

where  $D$  is liquid pool width. Typical values of Ma for weld pools are of the order of  $10^4$  or above.<sup>16)</sup>

**4. Results and Discussion**

Strip casting directly from a liquid melt pool was performed using an austenitic stainless steel containing different surface active elements. Edge serration amplitude or notch size were found to be dependent on the surface active elements present and also the Si and O<sub>2</sub> content of the melt. The origin of serrations and their initiation conditions were investigated considering three major instabilities mentioned above. The theoretical background given above and equations governing the

three different cases were used to make predictions for the initiation conditions and these were correlated with the experimental parameters. These were obtained by taking side photographs of the meniscus and the developing strip from the melt pool, and the measuring the surface tension of the test alloy using a levitated droplet method.<sup>17)</sup>

The theoretical calculations to predict the Kelvin-Helmholtz instability condition from Eq. (7) yields a critical velocity difference  $V_1 - V_2 = 22.9 \text{ m s}^{-1}$  between liquid stainless steel and air assuming the density of stainless steel  $\rho_1 = 7100 \text{ kg m}^{-3}$  and air density  $\rho_2 = 1.293 \text{ kg m}^{-3}$ ,  $g = 9.8 \text{ m s}^{-2}$ , and the surface tension between liquid and air  $\sigma_{lv} = 1.4 \text{ N m}^{-1}$ . Theoretically, if the velocity difference exceeds  $22.9 \text{ m s}^{-1}$  Kelvin-Helmholtz instability may exist but melt overflow experiments were performed at not more than  $2.7 \text{ m s}^{-1}$  and instabilities were observed even at these velocities.

The stainless steel alloys were initially deoxidized by ferromanganese which resulted in a smooth edged strip compared to stainless steel deoxidized by ferrosilicon which gave rise to serrated edge strips in some experiments. The effect of viscosity can be considered here apart from the role of surface tension since Si lowers the viscosity of the alloy and this low viscosity may result in travelling instability waves instead of damping. Figure 3 shows the strips produced under different casting conditions in alloys containing different surface active concentrations.<sup>1,18)</sup>

#### 4.1. The Effect of Casting Speed on Strip Dimensions and Edge Quality

It has been observed that the optimum casting speed or liquid pressure which is more than the numerical value deduced from Eq. (1) behind the melt pool is effective

to prevent or wash away developing instability waves.

The strips on the right of Fig. 3 numbered E27, E24 having high edge serration sizes with negative  $\Delta V$  velocity difference values (the velocity difference between pouring velocity and theoretical minimum stream velocity values calculated from Eq. (1) correspond to the runs with slow casting speeds which is insufficient to prevent melt instabilities. On the contrary the strips on the left of the figure have smooth edges produced at sufficiently high casting speeds results in a positive  $\Delta V$  which is effective in suppressing growing instabilities.

The strips of alloys with high concentrations of surface active elements have more serrations on the edges. These serrations may also originate from variations in the thickness, composition and strength of the solid oxide skin as proposed by Schwabe and co-workers.<sup>19)</sup> This may be due to the oxide on the liquid suppressing the surface tension driven flow and hence damping subsequent instabilities.

The final strip depends on:

(1)  $\Delta V$  (This can be calculated from Eq. (6) necessary to wash away instabilities. Figure 3 shows how the  $\Delta V$  value effects the suppression of instabilities and serrations.

(2) Marangoni number, this should be small. This can not be observed easily since the suppression of Ma flow is also dependent on the surface film chemistry.

(3) Deoxidation, this controls the liquid surface film viscosity.

(4) The melt viscosity, this can be controlled by adjusting the superheat, silicon and sulphur content of alloy.

#### 4.2. The Role of Surface Tension on Melt Drag

The condition of strip formation pulling the liquid

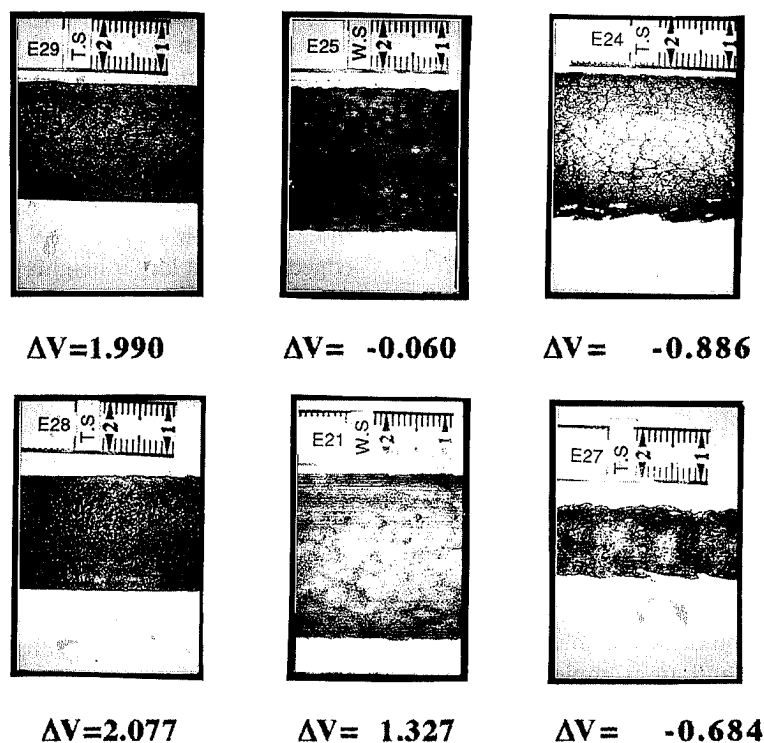


Fig. 3. Strips produced under different casting conditions and containing different surface active concentrations.

**Table 1.** The alloy characteristics, strip and serration dimensions of various runs.

%S**	$\frac{d\sigma}{dT}$ $\times 10^3$ (N/m <sup>2</sup> °C)	$\sigma$ (N/m)	Description of strip edge and surface quality	Width (mm)			Edge notch size Se (mm)	
				Min	Mean	Max		
0.0122	1.010	2.09	Low oxide on surface	28.3	28.5	29	0.7-1	1
0.0127	0.814	2.15	Low oxide on surface	29	29.5	30	0.5-0	1
0.0150	0.973	2.02	Low oxide, uniform edge	20	20	20	0.001	2
0.0170	1.359	1.93	Oxide, voids, serrated edge	11	11.5	12	1.2-1	2
0.0181	-0.062	2.04	Low oxide, uniform edge	7	7	7	0.1-0	2
0.0189	1.362	2.01	Non uniform width	4	5	6	0.05-0	1
0.0195	1.479	1.97	Uniform width, voids, serrated edge	22	26	30	1	2
0.0203	1.215	1.95	Uniform width, voids, serrated edge	22	26	30	1	2
0.0217	0.772	1.84	Uniform width, serrated edge	15	17.5	20	0.05-1.5	2
0.0224	0.957	1.85	Uniform width, serrated edge	15	17.5	20	0.05-1.5	2
0.0231	1.587	2.15	Low oxide, uniform edge	29	29.5	30	0.5-0	1
0.0232	1.529	1.99	Low oxide, uniform edge	32	33	34	0.01-0	2
0.0268	0.425	1.72	Uniform width, some voids	26	27	28	0.05-0.01	2
0.0272	0.643	1.67	Uniform width, some voids	26	27	28	0.05-0.01	2
0.0361	0.355	1.58	Uniform width, serrated edge	5	5.5	6	1.6-1	2
0.0382	0.449	1.68	Voids serrated edge	20	22.5	25	0.01	2
0.0736	1.224	1.43	Oxide on surface, uniform	25	30	35	2	1
0.0901	0.780	1.43	Oxide on surface, uniform	25	30	35	2	1
0.382	0.777	1.12	Voids, serrated edge, oxidized	8	9	10	2-3	2

(1) Serration at one side. (2) Serration at both sides.

\*\* Sulphur in sample after surface tension measurements.

front in the lip was tested by investigating the limiting values of surface tension for series of stainless steel and a Metglass alloy (Ni-Si-B) having high surface tension and viscosity. Surface tension values greater than 2.4 N m<sup>-1</sup> prevent the surface of the liquid pool from dragging parallel to the momentum transfer by the wheel. Surface tension were varied by adding Al and FeSi to control dissolved oxygen control. High  $\sigma_v$  values such as 2.0-2.2 N m<sup>-1</sup> were observed when deoxidation resulted in final low oxygen concentration of 95 ppm O in stainless steel. For surface tension values lower than 2.1 N m<sup>-1</sup> almost every run could have produced some strips successfully, dragging the liquid metal from the pool. Strip characteristics and temperature coefficients are given in **Table 1**. For the surface tensions between 2.1 and 1.4 N m<sup>-1</sup>, uniform strips can be produced for wheel speed 2.78 m s<sup>-1</sup>. The results also demonstrate that  $\Delta V (= V_c - V_j)$  the speed difference of the experimental casting speed  $V_c$  and the theoretical speed  $V_j$  necessary to prevent instability waves defined in Eq. (1) is a capillary wave related criterion which can be utilized to explain saw edge formation. Yuhara and co-workers<sup>22)</sup> observed a similar edge saw formation in twin-roll process but they applied electromagnetic field which created Lorentz forces to suppress surface waves on the melt pool.

### 4.3. Meniscus Characteristics

Optical photography was used to examine the side view of melt overflow and the meniscus during processing. Meniscus and strip formation of 304 stainless steel strip casting were photographed and an example is shown in **Fig. 4**. Photographic enlargement was used to measure capillary radius for the melt overflow experiments for 304 stainless steel with different surface tension values.

The relationship between the strip thickness and the radius of curvature of the meniscus at its apparent point of contact with the wheel was obtained by regression analysis of the data and capillary numbers calculated.<sup>1)</sup> The result is

$$\frac{t}{R} = 2.83 \times 10^4 \times Ca^{2.93} \dots\dots\dots (11)$$

where  $t$  is the strip thickness,  $R$  is radius of curvature and  $Ca$  is capillary number. The exponent and constant of this equation are different than in the equation proposed<sup>20)</sup> for aqueous solutions this is due to the surface tension and viscosity values of liquid metals compare to aqueous solutions.

The liquid metal heights at the lip were found to be directly proportional to the pool length where the liquid metal is dragged out of the pool. This can be seen in **Fig. 5**. The liquid height decreased gradually toward the end of casting. Low heights (8-9 mm) generally yielded saw edged strip but larger heights between 14-16 mm yielded uniform strips. The width of strips varied between 9 and 30 mm.

The results revealed that the dimensionless liquid height (Lh) width (w) ratio for a series of stainless alloys with different surface tensions were in range 0.3-0.9. Good edge strips were produced under experimental conditions which had a ratio between 0.6-0.9. The measurements of liquid heights,<sup>1)</sup> surface tension of 304 stainless steels<sup>17)</sup> show that the Lh/w ratio is linearly proportional to the surface tension as shown in **Fig. 6**.

Melt pool shape observations on the side view photographs revealed that alloys having high surface tensions also have a large meniscus radius. These meniscus radius values were measured as 14.52 and 7.7 mm for surface tensions 1.98 and 1.43 N m<sup>-1</sup> respectively.

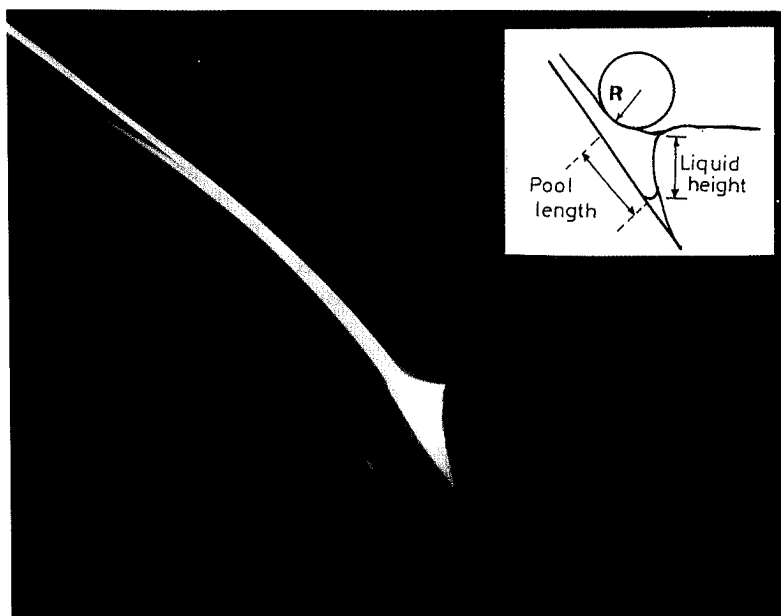


Fig. 4. *In situ* high speed photography of meniscus region during the melt overflow of stainless steel strip (1).

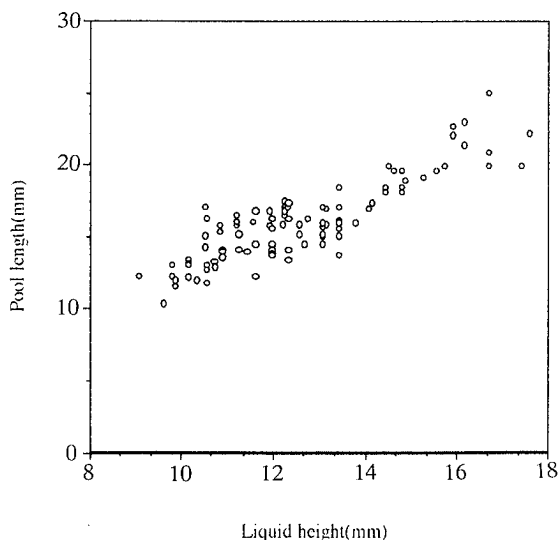


Fig. 5. The relationship between melt pool dimensions.

#### 4.4. Surface Tension and Melt Instabilities

Surface tension which is both temperature and compositionally dependent,<sup>21)</sup> measured were found to be related to the strip surface & edge quality. It is found that the temperature coefficient of surface tension has little direct relationship to edge quality but surface tension has a marked effect.<sup>1)</sup> In a ferrous alloy the Marangoni number is dependent on several factors such as temperature coefficient of surface tension, the temperature difference across the characteristic length (pouring channel width) over which Ma flow develops, viscosity and thermal diffusivity. But it is difficult to investigate the effects of these factors on serrations and viscosity independently. It is observed that a low viscosity and a low surface tension result in thin strip and edge serrations.

In melt overflow experiments the lip width was kept constant at 30 mm. It is found that increasing sulphur

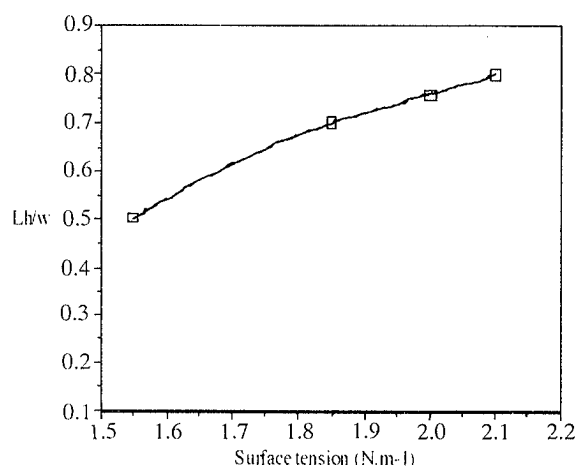


Fig. 6. The effect of surface tension on liquid height/width ratio.

and oxygen concentration reduced the absolute value of surface tension and increased the size of serrations and moreover resulted in Marangoni flow. The presence and severity of instabilities and their final effects on the strip were analyzed by considering  $\sigma_v$  for the system. Table 1 presents  $d\sigma/dT$  against serration size and variations in width. The Marangoni numbers calculated from Eq. (8) are between 247 000 and 57 850. The highest Marangoni number corresponds to a serrated edge strip with an edge notch size 1.2 mm and lowest Marangoni number 57 850 corresponds an edge notch size 0.05 mm. The extreme case revealed that there is consequence effect of high Marangoni number on strip edge characteristics because surface driven flow having large Ma number disturbs liquid pool surface like gas boundary interaction which may occur at the edges and boundary layer between liquid strip/wheel. Any disturbance may originate from liquid pool either from free surface or gas boundary between liquid and chiller causes travelling instability waves first in liquid then mush and finally solid strip.<sup>3)</sup>

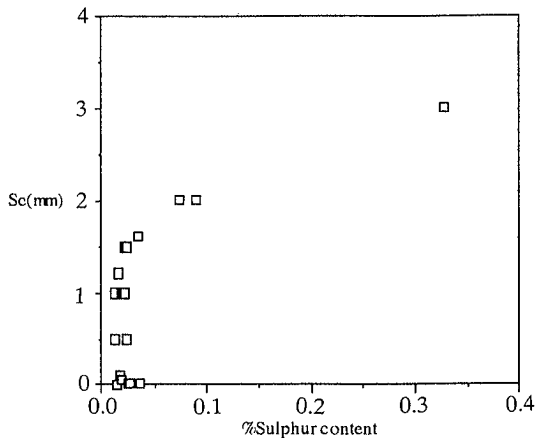


Fig. 7. The effect of sulphur concentration in 304 stainless steel alloy on serration notch size of strip.

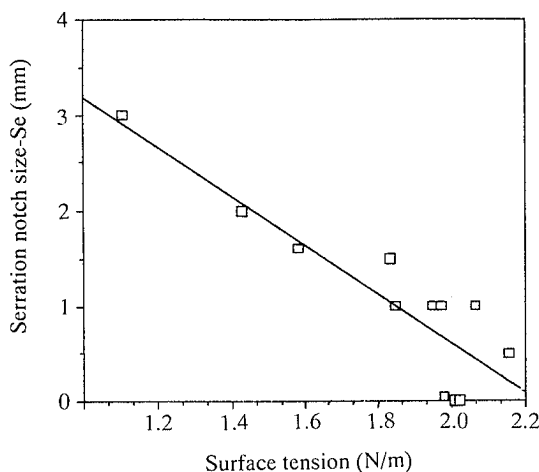


Fig. 8. The effect of melt surface tension on serration notch size.

A direct relationship of high sulphur concentration in 304 stainless steel alloy on the strip edge quality in terms of edge notch size  $S_e$  were observed and is given in Figs. 7 and 8. Decrease in surface energy with sulphur concentration resulted in high strip edge serration size.

## 5. Conclusions

(1) Direct strip casting from liquid metal is a casting operation which requires the control of alloy parameters such as surface tension, viscosity and melt superheat, and also operation parameters such as melt delivery speed, furnace channel length and the gap between pouring lip and rotary chiller.

(2) Edge serrations ranging from 0.05 to 1.2 mm originate from melt instabilities which occur as a result of liquid melt/gas boundary layer flow interactions.

(3) Three major instabilities may develop simultaneously, and they are difficult to isolate.

(4) No direct relationship was found between temperature coefficient of surface tension and the size of serrations. But extreme values of Marangoni number

(Ma) there is a linear variation of the serration notch size with Ma.

(5) The most severe instability waves were observed at the initial and final stages of strip formation.

(6) The absolute values of surface tension was observed to be an effective alloy parameter which can be related to the edge serration dimension.

(7) The difference between experimental casting speed and theoretical fluid flow velocity values were found to be directly proportional to the size of edge serrations.

(8) There is a critical lower casting speed which must be exceeded if successful strip is to be made. Otherwise there are critical ranges for operation and alloy characteristics.

## Acknowledgments

The authors wish to acknowledge for funding by The Open University and Fibre Technology, also for the help provided in various aspects by the staff of The Open University Walton Hall and the Oxford Research Unit, UK.

## REFERENCES

- 1) A. Kalkanli: Ph. D. Thesis, The O.U. Milton Keynes, UK, (1992).
- 2) Kavesh: Rapid Solidification Technology Source Book, ed. by R. L. Ashbrook, ASM, Metals Park, Ohio, (1976), 81.
- 3) T. R. Anthony and H. E. Cline: *J. Appl. Phys.*, **49** (1978), No. 2, 829.
- 4) V. G. Levich: *Physicochemical Hydrodynamics*, Ch1, Prentice Hall Inc., Englewood Cliffs., W55-3092, (1962), 378.
- 5) O. K. Brimacombe and F. Weiberg: *Metall. Trans. A*, **3** (1972), 2298.
- 6) G. K. Batchelor: *Fluid Mechanics*, University Printing House, Cambridge, (1970).
- 7) H. Rouse: *Elementary Mechanics of Fluids*, Wiley, New York, (1946).
- 8) M. Plateau: *Statique des Liquides*, University of Paris, (1873).
- 9) Rayleigh: *Joint Magnetism and Magnetic Materials*, Intermag Conf. AIP/IEEE, Pittsburgh, unpublished, (1976).
- 10) H. H. Liebermann and Graham: *Joint Magnetism and Magnetic Materials*, Intermag Conf. AIP/IEEE, Pittsburgh, unpublished, (1976), 21.
- 11) R. J. Hull: *Trans. ASME*, **111** (1989), May, 352.
- 12) Chang and Russell: *Phys. Fluids*, **8** (1965), 1018.
- 13) Nayfec and Saric: *J. Fluid Mech.*, **46** (1971), 209.
- 14) Chandrasekhar: *Hydrodynamic and Hydromagnetic Stability*, (1961).
- 15) Keene: *A Survey of Extant Data for the Surface Tension of Iron and Its Binary Alloys*, NPL Report DMA(A) 67, (1983), 1.
- 16) R. Zher, M. Chen and J. Mazumder: *Modelling of Casting and Welding Process IV*, (1988), 435.
- 17) A. Kalkanli, D. Grant, J. V. Wood and E. Selcuk: *High Temp. High Press.*, **25** (1994), 435.
- 18) Kordyban: *Hydrodynamic and Hydromagnetic Stability*, Dover. Publ ISBN 0-486-64071-X, (1977).
- 19) D. Schwabe, R. Lamprecht and A. Scharmann: *Physicochemical Hydrodynamics*, ed. by R. F. Probst, Butterworths, London, (1989), 291.
- 20) K. J. Ruschak: *Chem. Eng. Sci.*, **31** (1976), 1057.
- 21) G. R. Belton: *Metall. Trans.*, **7B** (1976), 35.
- 22) T. Yuhara, T. Kozuka, I. Muchi and S. Asai: *Casting of Near Net Shape Products*, ed. by Y. Sahai *et al.*, The Metallurgical Society, (1988).